

This is a non-peer reviewed preprint submitted to  
EarthArXiv



Subsequent peer-reviewed versions of this manuscript may have slightly different content. The authors welcome feedback.

<sup>†</sup>Corresponding email address: [sandy.herho@email.ucr.edu](mailto:sandy.herho@email.ucr.edu)

# Towards statistical modeling of chlorophyll-a concentrations in Balikpapan Bay, Indonesia: Implications for algal bloom detection

Iwan P. Anwar<sup>1, 2</sup>, Sandy H. S. Herho<sup>2, 3\*</sup>, Faruq Khadami<sup>1</sup>,  
Mutiarara R. Putri<sup>1</sup>, Sabitha C. Syahrial<sup>1</sup>

<sup>1</sup>Applied and Environmental Oceanography Research Group, Bandung Institute of Technology (ITB), Jalan Ganesha 10, Bandung, 40132, West Java, Indonesia.

<sup>2</sup>Samudera Sains Teknologi (SST) Ltd., Gang Sarimanah XIII/67, Bandung, 40151, West Java, Indonesia.

<sup>3\*</sup>Department of Earth and Planetary Sciences, Department of Earth and Planetary Sciences, University of California, 900 University Ave., Riverside, 92521, CA, USA.

\*Corresponding author(s). E-mail(s): [sandy.herho@email.ucr.edu](mailto:sandy.herho@email.ucr.edu);

## Abstract

This study presents a comprehensive statistical analysis of chlorophyll-a dynamics in Balikpapan Bay, Indonesia, combining time series analysis, extreme value modeling, and machine learning techniques to understand phytoplankton variability near Indonesia's planned new capital city. Analysis of daily chlorophyll-a concentrations (2019-2021) revealed a non-Gaussian distribution (skewness = 2.212, kurtosis = 10.160) ranging from 0.350 to 11.270 mg/m<sup>3</sup>, with distinct seasonal patterns showing May maxima (2.110 mg/m<sup>3</sup>) and July minima (1.340 mg/m<sup>3</sup>). Block Maxima extreme value analysis identified 79 extreme events and fitted a Gumbel distribution (location  $\mu = 2.924$ , scale  $\sigma = 1.231$ , log-likelihood = -141.644), though notably failed to capture two major HAB events (11.270 and 10.430 mg/m<sup>3</sup>). A WeightedEnsemble.L2 model combining ExtraTreesMSE (0.462), CatBoost (0.346), and LightGBMXT (0.192) identified temperature (importance: 0.072,  $p < 0.001$ ), solar radiation (0.061,  $p = 0.002$ ), and phosphate (0.047,  $p < 0.001$ ) as key drivers, achieving moderate performance (RMSE = 0.868 mg/m<sup>3</sup>,  $R^2 = 0.204$ ). The trained model was serialized for potential operational deployment, providing crucial baseline data for HAB monitoring systems in this rapidly developing coastal region.

**Keywords:** AutoGluon Machine Learning, Coastal Phytoplankton Dynamics, Extreme Value Analysis, Tropical Ecosystem Management

# 1 Introduction

The Indonesian government’s plan to relocate the national capital from Jakarta to Nusantara, situated in East Kalimantan province, has brought significant attention to the coastal ecosystems in the region [1]. Of particular importance is Balikpapan Bay, which will serve as the coastal area for the new capital city [2]. This semi-enclosed bay, oriented on a north-south axis and approximately 35 km long and 1-8 km wide, is poised to play a crucial role in the development and environmental management of the new capital [2, 3].

Balikpapan Bay is characterized by complex water mass dynamics influenced by various environmental factors, including the ocean dynamics of the Makassar Strait and freshwater inputs from several rivers [3–5]. The bay receives freshwater from four major rivers: Sepaku, Semoi, Wain, and Riko, while saline water enters from the Makassar Strait via the bay’s mouth [6, 7]. These hydrodynamic processes are further modulated by diurnal and seasonal rainfall variations, with wet seasons typically occurring from November to December and March to April, and the dry season from August to October [8, 9].

The water mass dynamics in Balikpapan Bay have been shown to significantly impact water quality, phytoplankton abundance, chlorophyll-a concentration, and other marine bio-geophysical parameters [10, 11]. The prevailing semidiurnal tide type in the bay contributes to increased phytoplankton abundance and nutrient distribution within the water column [12, 13]. However, the bay’s ecosystem is also under pressure from various anthropogenic factors, including oil spills, domestic and industrial waste, and agricultural activities [6, 14, 15].

The relocation of Indonesia’s capital to Nusantara is expected to bring about significant changes to the region, potentially increasing environmental pressures on Balikpapan Bay. As the new capital city develops, there is a substantial risk of increased nutrient enrichment from domestic and industrial sources [16]. This nutrient loading, combined with the bay’s unique hydrodynamics, could potentially lead to eutrophication and harmful algal blooms (HABs), which pose serious threats to marine ecosystems and human health [17, 18].

Given the ecological importance of Balikpapan Bay and its proximity to the future capital, there is an urgent need to understand the bay’s current environmental status and its potential responses to increased anthropogenic pressures. While extensive research has been conducted on HABs in other Indonesian bays, such as Jakarta [19, 20], Lampung [21, 22], and Ambon [23, 24], studies specific to Balikpapan Bay are limited. However, there is suspected evidence of algal bloom occurrences and the presence of HAB-causing phytoplankton species in the bay [4].

In light of these concerns and Balikpapan Bay’s newfound significance, this study aims to investigate the variability of chlorophyll-a concentration, a key indicator of phytoplankton biomass and potential HABs. We analyze ocean color reanalysis

data, hydrodynamic model outputs, and various environmental parameters to identify patterns in chlorophyll-a distribution, detect potential algal bloom events, and explore relationships between chlorophyll-a concentration and environmental factors. Our methodology employs a comprehensive statistical approach, including exploratory data analysis and time series analysis. We utilize a threshold-based approach to identify algal bloom events, following previous research with modifications based on our data comparison. Additionally, we leverage machine learning techniques, specifically the AutoGluon framework [25, 26], to capture complex, non-linear relationships in the ecological data. This approach allows us to model interactions between chlorophyll-a concentrations and various environmental parameters, with feature importance analysis identifying the most influential factors. By combining these statistical methods with comprehensive environmental data, we aim to provide a nuanced understanding of the dynamics governing chlorophyll-a concentrations and potential algal bloom events in Balikpapan Bay, contributing to effective management strategies for this critical ecosystem as Indonesia’s new capital city takes shape.

## 2 Data and Methods

### 2.1 Data

This study focuses on Balikpapan Bay, Indonesia (116.7°E, 1.0°S, Fig. 2.2.5), utilizing data from January 1, 2019, to December 31, 2021, as previously analyzed by Anwar et al. [27]. The primary dataset comprises daily chlorophyll-a concentrations derived from ocean color reanalysis data (OCEANCOLOUR\_GLO\_BGC\_L4\_MY\_009\_104) provided by the Copernicus Marine Environment Monitoring Service (CMEMS) [28].

The data used in this study are spatially averaged over the Balikpapan Bay area and presented at a daily resolution. Spatial averaging is employed to provide a representative overview of the entire bay ecosystem, reducing the impact of local variability and allowing for a more generalized analysis of chlorophyll-a dynamics [31]. This approach is particularly useful in coastal areas where small-scale spatial heterogeneity can be high due to complex interactions between terrestrial inputs, ocean currents, and local bathymetry [32].

The daily resolution of the data allows for the capture of short-term variability in chlorophyll-a concentrations and associated environmental parameters. This temporal scale is crucial for identifying rapid changes in phytoplankton biomass that can occur in response to environmental fluctuations, such as nutrient pulses from river discharge events or short-term changes in meteorological conditions [33]. Daily data also enable the detection of phenomena such as algal blooms, which can develop and dissipate over the course of days to weeks [34].

To comprehensively analyze the factors influencing chlorophyll-a dynamics, we incorporated several additional environmental parameters. Sea surface temperature (SST) and salinity (SSS) data were obtained from the Hamburg Shelf Ocean Model (HAMSOM) [4]. SST and SSS play crucial roles in phytoplankton growth and distribution [35, 36]. River discharge data were sourced from the Global Flood Awareness System (GloFAS-ERA5) [37]. River inputs significantly affect coastal nutrient dynamics and, consequently, phytoplankton growth [38, 39].



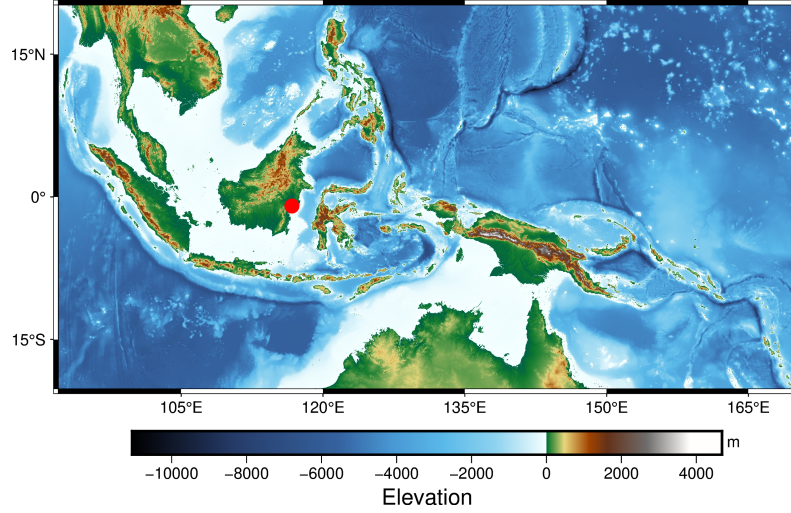


**Fig. 1:** Location map of the study area showing bathymetry and topography of Maritime Southeast Asia from SRTM15+ Earth Relief v2.6 data [29]. The red dot indicates the location of Balikpapan Bay ( $116.71^{\circ}\text{E}$ ,  $-0.97^{\circ}\text{N}$ ). Elevation and depth are shown in meters, with positive values (green to white) representing land topography and negative values (blue) representing ocean bathymetry. Map generated using PyGMT [30].

Nitrate, phosphate, silicate, and dissolved oxygen data were acquired from the Global Ocean Biogeochemistry Analysis and Forecast (GLOBAL\_ANALYSIS\_FORECAST\_BIO\_001\_028) [40]. These nutrients are essential for phytoplankton growth and can limit primary productivity in marine ecosystems [41, 42]. Solar radiation data were obtained from ERA5 hourly data, which were accumulated into daily totals [43]. This daily accumulation provides a more appropriate temporal scale for analyzing the impact of light availability on photosynthesis and phytoplankton growth [44, 45]. Rainfall data were collected from BMKG Sepinggan station, Balikpapan [46]. Precipitation can influence nutrient input through runoff and affect water column stability, both of which impact phytoplankton dynamics [47, 48].

This multi-faceted approach, combining spatially averaged, daily resolution data from various sources, provides a comprehensive framework for analyzing the complex interactions between physical, chemical, and biological processes that govern chlorophyll-a dynamics in Balikpapan Bay. It allows for the investigation of both short-term variability and longer-term trends, crucial for understanding coastal ecosystem functioning in the context of climate change and anthropogenic influences [49, 50].

## 2.2 Methods

Our analysis of chlorophyll-a dynamics in Balikpapan Bay employed a multi-faceted approach, combining exploratory data analysis, time series analysis, extreme value

analysis, and machine learning techniques. This comprehensive methodology was chosen to capture the complex nature of coastal marine ecosystems, where multiple environmental factors interact to influence phytoplankton dynamics [51, 52].

### 2.2.1 Exploratory Data Analysis

We began with exploratory data analysis on the chlorophyll-a concentration time series. Basic descriptive statistics were computed, including mean ( $\mu$ ), standard deviation ( $\sigma$ ), minimum, maximum, and quartiles. The mean and standard deviation were calculated using the following equations:

$$\mu = \frac{1}{N} \sum_{t=1}^N X_t \quad (1)$$

$$\sigma = \sqrt{\frac{1}{N-1} \sum_{t=1}^N (X_t - \mu)^2} \quad (2)$$

where  $X_t$  represents the chlorophyll-a concentration at time  $t$ , and  $N$  is the total number of observations [53]. These basic statistics provide an initial understanding of the central tendency and variability in the data, which is crucial for identifying potential patterns or anomalies in chlorophyll-a concentrations [54].

To assess the distribution's shape, we calculated skewness ( $S$ ) and kurtosis ( $K$ ):

$$S = \frac{1}{N} \sum_{t=1}^N \left( \frac{X_t - \mu}{\sigma} \right)^3 \quad (3)$$

$$K = \frac{1}{N} \sum_{t=1}^N \left( \frac{X_t - \mu}{\sigma} \right)^4 - 3 \quad (4)$$

These measures provide insights into the asymmetry and tailedness of the distribution, respectively [55]. Understanding the distribution shape is particularly important in marine ecosystems, where skewed distributions of chlorophyll-a are common due to episodic bloom events [56].

### 2.2.2 Normality and Stationarity Tests

We employed the Shapiro-Wilk test [57] and D'Agostino's  $K^2$  test [58] to evaluate the normality of the chlorophyll-a distribution. The Shapiro-Wilk test statistic is given by:

$$W = \frac{(\sum_{i=1}^n a_i x_{(i)})^2}{\sum_{i=1}^n (x_i - \bar{x})^2} \quad (5)$$

Where  $x_{(i)}$  are the ordered sample values and  $a_i$  are constants derived from the covariances of the order statistics. The null hypothesis of this test is that the sample comes from a normally distributed population. We reject this hypothesis if the p-value is less than the chosen alpha level.

D'Agostino's  $K^2$  test combines skewness ( $S$ ) and kurtosis ( $K$ ) to produce an omnibus test of normality:

$$K^2 = Z_1(S)^2 + Z_2(K)^2 \quad (6)$$

Where  $Z_1(S)$  and  $Z_2(K)$  are approximately standard normal under the null hypothesis of normality. The test statistic  $K^2$  follows a chi-square distribution with two degrees of freedom under the null hypothesis.

These tests are crucial because many statistical methods assume normality, and violations of this assumption can lead to incorrect inferences [59].

To assess the stationarity of the time series, we used the Augmented Dickey-Fuller (ADF) test [60] and the Kwiatkowski-Phillips-Schmidt-Shin (KPSS) test [61].

The ADF test is based on the regression model:

$$\Delta Y_t = \alpha + \beta t + \gamma Y_{t-1} + \sum_{i=1}^p \delta_i \Delta Y_{t-i} + \epsilon_t \quad (7)$$

Where  $\Delta Y_t$  is the differenced series,  $\alpha$  is a constant,  $\beta$  is the coefficient on a time trend,  $\gamma$  is the coefficient of interest for testing stationarity,  $p$  is the lag order of the autoregressive process, and  $\epsilon_t$  is the error term. The null hypothesis of the ADF test is that the time series contains a unit root (i.e., it is non-stationary). The test statistic is:

$$ADF = \frac{\hat{\gamma}}{SE(\hat{\gamma})} \quad (8)$$

Where  $\hat{\gamma}$  is the estimate of  $\gamma$  and  $SE(\hat{\gamma})$  is its standard error.

The KPSS test, in contrast, has stationarity as the null hypothesis. It is based on the model:

$$Y_t = \xi t + r_t + \epsilon_t \quad (9)$$

Where  $\xi t$  is a deterministic trend,  $r_t$  is a random walk, and  $\epsilon_t$  is a stationary error. The test statistic is:

$$KPSS = \frac{\sum_{t=1}^T S_t^2}{T^2 \hat{f}_0} \quad (10)$$

where  $S_t = \sum_{i=1}^t \hat{\epsilon}_i$  is the partial sum of residuals,  $T$  is the sample size, and  $\hat{f}_0$  is an estimator of the spectral density at frequency zero.

Stationarity is a key assumption in many time series analyses, and its violation can indicate the presence of trends or seasonal patterns in chlorophyll-a concentrations [62]. By using both ADF and KPSS tests, we can differentiate between trend-stationary and difference-stationary processes, providing a more comprehensive assessment of the time series properties.

### 2.2.3 Autocorrelation Analysis

We computed and plotted the Autocorrelation Function (ACF) and Partial Autocorrelation Function (PACF) to examine the temporal dependence structure of the chlorophyll-a time series. These functions provide crucial insights into the underlying stochastic processes governing phytoplankton dynamics [63].

Let  $\{X_t\}$  be a weakly stationary time series with mean  $\mu$  and variance  $\sigma^2$ . The autocovariance function at lag  $k$  is defined as:

$$\gamma(k) = \mathbb{E}[(X_t - \mu)(X_{t+k} - \mu)] \quad (11)$$

The Autocorrelation Function (ACF) is the normalized version of the autocovariance function:

$$\rho(k) = \frac{\gamma(k)}{\gamma(0)} = \frac{\mathbb{E}[(X_t - \mu)(X_{t+k} - \mu)]}{\mathbb{E}[(X_t - \mu)^2]} \quad (12)$$

For a finite sample of size  $N$ , we estimate the ACF using:

$$\hat{\rho}(k) = \frac{\sum_{t=1}^{N-k} (X_t - \bar{X})(X_{t+k} - \bar{X})}{\sum_{t=1}^N (X_t - \bar{X})^2} \quad (13)$$

where  $\bar{X}$  is the sample mean.

The Partial Autocorrelation Function (PACF) measures the correlation between  $X_t$  and  $X_{t+k}$  after removing the linear dependence on the intervening variables  $X_{t+1}, \dots, X_{t+k-1}$ . It is defined as:

$$\alpha(k) = \text{Corr}(X_t, X_{t+k} | X_{t+1}, \dots, X_{t+k-1}) \quad (14)$$

The PACF can be computed recursively using the Durbin-Levinson algorithm:

$$\alpha(1) = \rho(1) \quad (15)$$

$$\alpha(k) = \frac{\rho(k) - \sum_{j=1}^{k-1} \alpha_{k-1,j} \rho(k-j)}{1 - \sum_{j=1}^{k-1} \alpha_{k-1,j} \rho(j)} \quad (16)$$

where  $\alpha_{k,j}$  are the coefficients in the projection of  $X_t$  onto the space spanned by  $X_{t-1}, \dots, X_{t-k}$ .

For a stationary AR(p) process, the theoretical PACF has the following property:

$$\alpha(k) = \begin{cases} \neq 0 & \text{for } k \leq p \\ = 0 & \text{for } k > p \end{cases} \quad (17)$$

This property is particularly useful for order selection in autoregressive models.

We also consider the asymptotic distribution of the sample ACF for a white noise process. Under the null hypothesis that the true ACF is zero beyond a certain lag  $q$ , the sample ACF is approximately normally distributed:

$$\sqrt{N}(\hat{\rho}(k) - \rho(k)) \sim N(0, 1) \quad \text{for } k > q \quad (18)$$

This result allows us to construct confidence intervals and perform hypothesis tests on the significance of autocorrelations at various lags.

Autocorrelation analysis is particularly useful in studying phytoplankton dynamics, as it can reveal cyclical patterns and the persistence of bloom events [64]. The ACF can identify seasonal patterns and long-term dependencies, while the PACF can help in determining the order of autoregressive processes that might be driving the chlorophyll-a dynamics.

Moreover, the decay rate of the ACF can provide insights into the memory of the system. A slow decay might indicate long-range dependence, which has been observed in some ecological time series and can have important implications for forecasting and understanding ecosystem resilience [65].

#### 2.2.4 Extreme Value Analysis

We performed Extreme Value Analysis using the Block Maxima (BM) approach [66, 67]. This method is well-suited for analyzing extreme chlorophyll-a events, which are often associated with HABs [68].

Let  $X_1, X_2, \dots, X_n$  be a sequence of independent and identically distributed random variables with a common distribution function  $F$ . Define  $M_n = \max\{X_1, \dots, X_n\}$  as the maximum of this sequence. The distribution of  $M_n$  can be derived as:

$$P(M_n \leq z) = P(X_1 \leq z, \dots, X_n \leq z) = [F(z)]^n \quad (19)$$

As  $n \rightarrow \infty$ , this distribution degenerates to a point mass at the upper end point of  $F$ . To obtain a non-degenerate limiting distribution, we can normalize  $M_n$ :

$$P\left(\frac{M_n - b_n}{a_n} \leq z\right) = [F(a_n z + b_n)]^n \rightarrow G(z) \quad (20)$$

where  $a_n > 0$  and  $b_n$  are sequences of constants, and  $G$  is a non-degenerate distribution function. The Extremal Types Theorem states that if such a  $G$  exists, it must be one of three types: Gumbel, Fréchet, or Weibull. These three distributions can be combined into a single family, the Generalized Extreme Value (GEV) distribution:

$$G(z) = \exp\{-[1 + \xi((z - \mu)/\sigma)]^{-1/\xi}\} \quad (21)$$

defined on  $\{z : 1 + \xi(z - \mu)/\sigma > 0\}$ , where  $\mu \in \mathbb{R}$  is the location parameter,  $\sigma > 0$  is the scale parameter, and  $\xi \in \mathbb{R}$  is the shape parameter. The shape parameter  $\xi$  determines the type of distribution:

- $\xi > 0$ : Fréchet distribution (heavy upper tail)
- $\xi < 0$ : Weibull distribution (bounded upper tail)
- $\xi \rightarrow 0$ : Gumbel distribution (light upper tail)

We fitted the GEV distribution using the Markov Chain Monte Carlo (MCMC) method implemented in the pyextremes package [69]. The Metropolis-Hastings algorithm was used with 500 walkers and 2,500 samples per walker. This Bayesian approach allows for a more robust estimation of parameters, particularly useful when dealing with limited data on extreme events [70].

The MCMC algorithm generates samples from the posterior distribution  $p(\theta|x)$ , where  $\theta = (\mu, \sigma, \xi)$  are the GEV parameters and  $x$  is the observed data. The posterior is proportional to the product of the likelihood and the prior:

$$p(\theta|x) \propto L(x|\theta)p(\theta) \quad (22)$$

where  $L(x|\theta)$  is the likelihood function and  $p(\theta)$  is the prior distribution. The likelihood for the GEV distribution is:

$$L(x|\theta) = \prod_{i=1}^n \frac{1}{\sigma} [1 + \xi(\frac{x_i - \mu}{\sigma})]^{-1-1/\xi} \exp\{-[1 + \xi(\frac{x_i - \mu}{\sigma})]^{-1/\xi}\} \quad (23)$$

Return periods were calculated using:

$$T(z) = \frac{1}{1 - G(z)} \quad (24)$$

where  $T(z)$  is the return period for the value  $z$ . The return level  $z_p$  associated with the return period  $1/p$  is:

$$z_p = \begin{cases} \mu - \frac{\sigma}{\xi} [1 - (-\ln(1-p))^{-\xi}] & \xi \neq 0 \\ \mu - \sigma \ln(-\ln(1-p)) & \xi = 0 \end{cases} \quad (25)$$

Return period analysis is crucial for coastal management, providing insights into the frequency of potentially HABs [71].

This approach to extreme value analysis, combining theoretical foundations with Bayesian inference, allows for a robust characterization of extreme chlorophyll-a events, accounting for uncertainty in parameter estimation and providing a framework for risk assessment in coastal ecosystems.

### 2.2.5 Machine Learning

We employed the AutoGluon framework [25] for automated machine learning, leveraging its ability to handle complex, non-linear relationships often present in ecological data [72]. Let  $\mathcal{D} = \{(\mathbf{x}_i, y_i)\}_{i=1}^N$  be our dataset, where  $\mathbf{x}_i \in \mathbb{R}^d$  are the input features (including nitrate, phosphate, silicate, dissolved oxygen, total river discharge, rainfall, temperature, salinity, and solar radiation) and  $y_i \in \mathbb{R}$  is the target variable (chlorophyll-a concentration). We split  $\mathcal{D}$  into training and test sets,  $\mathcal{D}_{\text{train}}$  and  $\mathcal{D}_{\text{test}}$ , using an 80:20 ratio to ensure model generalizability [73].

AutoGluon employs an ensemble of diverse models  $\{f_k\}_{k=1}^K$ , including neural networks, gradient boosting machines, and random forests. The final prediction is a weighted average:

$$\hat{y} = \sum_{k=1}^K w_k f_k(\mathbf{x}) \quad (26)$$

where  $w_k$  are learned weights. The optimization problem can be formulated as:

$$\min_{\{f_k\}, \{w_k\}} \mathcal{L}(\{f_k\}, \{w_k\}) + \lambda \Omega(\{f_k\}, \{w_k\}) \quad (27)$$

where  $\mathcal{L}$  is the loss function,  $\Omega$  is a regularization term, and  $\lambda$  is a hyperparameter controlling the strength of regularization.

We evaluated the model using various metrics, including Root Mean Squared Error (RMSE):

$$\text{RMSE} = \sqrt{\frac{1}{n} \sum_{i=1}^n (y_i - \hat{y}_i)^2} \quad (28)$$

where  $y_i$  are the observed values and  $\hat{y}_i$  are the predicted values. RMSE is particularly useful in environmental modeling as it provides an interpretable measure of prediction accuracy in the same units as the response variable [74].

Feature importance was calculated using permutation importance:

$$FI_j = \frac{1}{K} \sum_{k=1}^K \mathcal{L}(y, f(\mathbf{X}^{(j,k)})) - \mathcal{L}(y, f(\mathbf{X})) \quad (29)$$

where  $\mathcal{L}$  is the loss function,  $f$  is the trained model,  $\mathbf{X}$  is the feature matrix,  $\mathbf{X}^{(j,k)}$  is the feature matrix with feature  $j$  permuted in repetition  $k$ , and  $K$  is the number of repetitions [75]. This technique helps identify the most influential environmental factors (such as nitrate, phosphate, silicate, etc.) driving chlorophyll-a dynamics, crucial for understanding and managing coastal ecosystems [76]. The statistical significance of feature importance can be assessed using a permutation test:

$$p_j = \frac{1}{M} \sum_{m=1}^M \mathbb{I}(FI_j^{(m)} \geq FI_j) \quad (30)$$

where  $FI_j^{(m)}$  are permuted feature importance values and  $M$  is the number of permutations.

To ensure reproducibility, we employed the Python ‘pickle’ module to serialize and deserialize the trained model. The serialization process can be represented as:

$$S : \mathcal{M} \rightarrow \mathcal{B} \quad (31)$$

where  $\mathcal{M}$  is the model space and  $\mathcal{B}$  is the binary file space. The deserialization process is the inverse:

$$D : \mathcal{B} \rightarrow \mathcal{M} \quad (32)$$

such that  $D(S(m)) = m$  for any model  $m \in \mathcal{M}$ . This allows us to save the trained model to a file and later reconstruct it exactly, ensuring consistent predictions across different environments or time points.

The pickle file contains not only the model parameters but also the entire model structure, including the ensemble architecture and individual model hyperparameters. This comprehensive serialization ensures that all aspects of the model, including feature preprocessing steps and the weighted ensemble structure, are preserved.

To further enhance reproducibility, we recorded the random seed used for data splitting and model initialization. Specifically, we set the random seed to 42. This seed value, when combined with the pickle file, allows for perfect replication of our results.

This machine learning approach, combined with our time series analysis and extreme value modeling, provides a robust framework for analyzing chlorophyll-a concentrations and their relationships with environmental parameters in Balikpapan Bay. By capturing both overall trends and extreme events in chlorophyll-a dynamics, we offer valuable insights for coastal management and ecosystem health assessment [77], with the added benefit of full reproducibility through our serialization approach.

### 3 Results and Discussion

The analysis of chlorophyll-a concentrations in Balikpapan Bay from 2019 to 2021 revealed complex temporal dynamics and environmental relationships across multiple time scales. Our findings progress from basic temporal patterns through advanced statistical characterizations to predictive modeling, providing insights into both typical conditions and extreme events in this tropical coastal system.

#### 3.1 Time Series Characteristics

The daily chlorophyll-a time series (Fig. 2) exhibited substantial variability, ranging from 0.350 to 11.270 mg/m<sup>3</sup>, with a mean of 1.757 mg/m<sup>3</sup> (SD = 1.099). This range exceeds typical values reported for similar tropical coastal systems [20], suggesting unique local forcing mechanisms. Two exceptional bloom events were recorded: 11.270 mg/m<sup>3</sup> on June 16, 2020, and 10.430 mg/m<sup>3</sup> on November 9, 2019, both exceeding the 99.9th percentile (5.87 mg/m<sup>3</sup>) of the distribution. These events significantly exceeded typical concentrations, representing potential HABs that warrant particular attention in the context of coastal management [34].

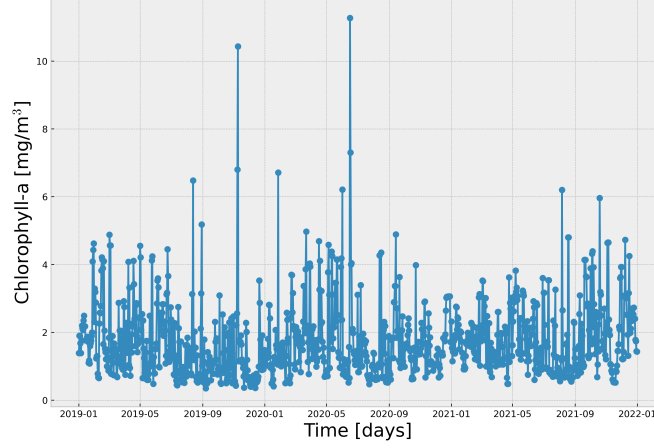


**Fig. 2:** Time series of daily chlorophyll-a concentrations in Balikpapan Bay (2019-2021). Daily observations are shown as points, with the two major HAB events highlighted (11.270 mg/m<sup>3</sup> on June 16, 2020, and 10.430 mg/m<sup>3</sup> on November 9, 2019)

Descriptive statistics revealed a positively skewed (2.212) and leptokurtic (10.160) distribution, characteristic of biological populations subject to multiplicative growth processes. The first quartile (1.000 mg/m<sup>3</sup>), median (1.510 mg/m<sup>3</sup>), and third quartile (2.180 mg/m<sup>3</sup>) describe the typical range during non-bloom conditions [78]. This



structure indicates that while the system maintains relatively stable background conditions most of the time, it is prone to occasional rapid increases in biomass that may represent significant ecological events.

The temporal pattern shows evidence of both regular and irregular fluctuations, with the extreme events occurring during different seasons (June and November). This timing suggests that bloom formation may be driven by episodic rather than purely seasonal forcing mechanisms [79]. The irregular spacing of extreme events indicates that simple seasonal or tidal cycles alone cannot explain the occurrence of high biomass events, pointing to the need for considering multiple environmental drivers in bloom prediction efforts.

### 3.2 Seasonal and Statistical Patterns

The seasonal analysis (Fig. 3) revealed distinct intra-annual patterns in chlorophyll-a concentrations, with maximum values occurring in May ( $2.110 \text{ mg/m}^3$ ) and minimum values in July ( $1.340 \text{ mg/m}^3$ ). This seasonal amplitude of  $0.770 \text{ mg/m}^3$  represents approximately 44% of the annual mean concentration, indicating substantial intra-annual variability. The timing of peak concentrations coincides with the transition period between the northwest and southeast monsoons, suggesting a strong influence of regional climate patterns on phytoplankton dynamics.

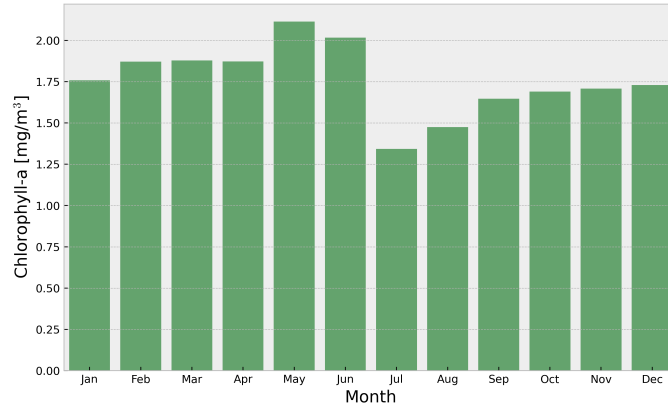


**Fig. 3:** Monthly average chlorophyll-a concentrations in Balikpapan Bay. This graphic demonstrates the highest concentrations in May ( $2.110 \text{ mg/m}^3$ ) and lowest in July ( $1.340 \text{ mg/m}^3$ )

The monthly progression exhibits an asymmetric pattern, with a relatively rapid increase from March to May followed by a more gradual decline into July. This asymmetry in the seasonal cycle suggests different mechanisms controlling the development and decline phases of phytoplankton populations [80]. The pre-peak acceleration phase might be driven by increasing light availability and water column stability, while

the post-peak decline could reflect a combination of nutrient depletion and increased grazing pressure.

The probability distribution of chlorophyll-a concentrations (Fig. 4) exhibited marked departures from normality, confirmed by both Shapiro-Wilk and D’Agostino’s  $K^2$  tests ( $p < 0.001$ ). The strong positive skewness (2.212) and high kurtosis (10.160) reflect the episodic nature of phytoplankton blooms and the multiplicative processes governing population growth [78]. This asymmetric distribution is particularly relevant for understanding the frequency and magnitude of potential HABs in the system.

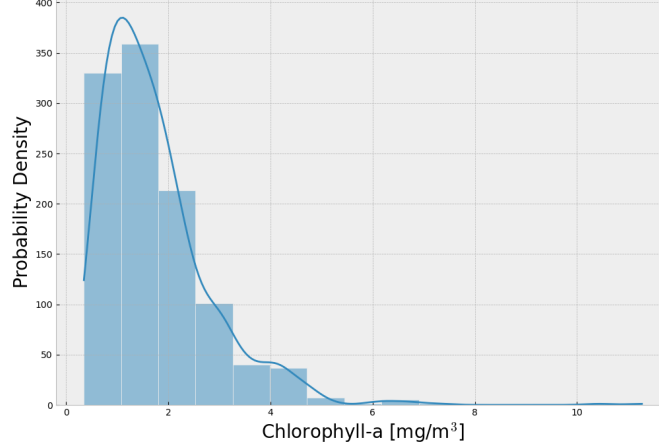


**Fig. 4:** Distribution of chlorophyll-a concentrations with kernel density estimation. The distribution shows strong positive skewness (2.212) and high kurtosis (10.160), characteristic of phytoplankton dynamics in coastal systems

The distribution shows a primary mode around the median (1.510  $\text{mg}/\text{m}^3$ ), with a pronounced right tail extending beyond 11  $\text{mg}/\text{m}^3$ . This structure suggests two distinct regimes: a stable background state characterized by moderate concentrations and controlled by regular environmental forcing, and an extreme state associated with bloom conditions that may arise from the alignment of multiple favorable growth factors [81]. The gap between the 75th percentile (2.180  $\text{mg}/\text{m}^3$ ) and the maximum observed value (11.270  $\text{mg}/\text{m}^3$ ) underscores the exceptional nature of bloom events in this system.

The kernel density estimation reveals subtle features in the distribution that might reflect distinct environmental states or phytoplankton community compositions. Multiple small peaks in the density curve suggest potential sub-populations or different ecological regimes that could correspond to varying combinations of environmental conditions [82]. This complex distribution structure has important implications for modeling approaches, suggesting that simple parametric models may not adequately capture the full range of variability in the system.

### 3.3 Temporal Correlation Structure

The temporal dependence analysis through autocorrelation functions (Fig. 5) revealed significant persistence in chlorophyll-a concentrations. The ACF exhibits a gradual decay pattern with significant positive correlations extending to approximately 15 days, indicating that biomass patterns typically persist for about two weeks. The slow decay in autocorrelation suggests that the system possesses significant memory, where current conditions influence future states through both direct biological processes and environmental persistence.

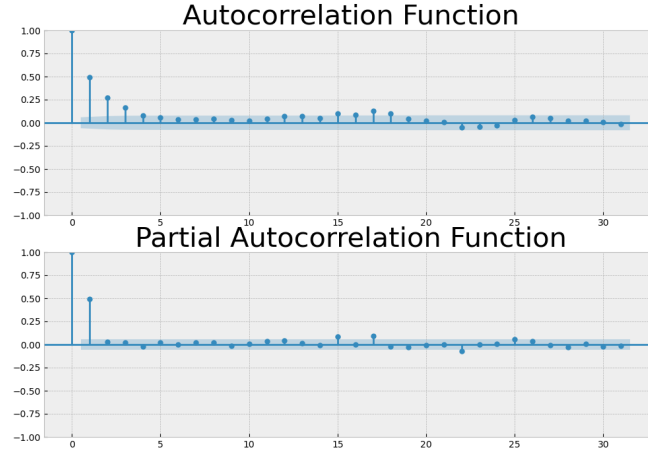


**Fig. 5:** Autocorrelation (ACF) and Partial Autocorrelation (PACF) functions for chlorophyll-a time series. Blue shading indicates 95% confidence intervals, showing significant temporal dependence extending to approximately 15 days

The PACF analysis revealed strong correlation at lag-1 (0.72) and significant but decreasing correlations at subsequent lags, particularly at 7 and 14 days. This pattern indicates both short-term persistence in daily concentrations and the influence of weekly to fortnightly cycles on chlorophyll-a dynamics. The lag-7 and lag-14 correlations suggest the importance of weekly and fortnightly tidal cycles in modulating phytoplankton biomass, a finding particularly relevant for coastal systems where tidal forcing plays a crucial role in nutrient dynamics and water column stability.

The correlation structure provides important insights for monitoring program design and bloom prediction efforts. The two-week persistence of significant correlations suggests that sampling intervals shorter than two weeks are necessary to capture the full dynamics of the system, particularly during bloom development phases. Moreover, the identified periodic components at weekly and fortnightly scales indicate that monitoring efforts should account for tidal phase in interpreting chlorophyll-a measurements [83].

### 3.4 Extreme Value Analysis

The extreme value analysis using the Block Maxima approach with a 14-day block size identified 79 extreme events over the study period. The fitted GEV distribution converged to a Gumbel distribution with location parameter  $\mu = 2.924$  and scale parameter  $\sigma = 1.231$ , as evidenced by the MCMC analysis using 500 walkers and 2,500 samples per walker (log-likelihood = -141.644, AIC = 287.446). However, critically, this model failed to capture the two most extreme HAB events (11.270 and 10.430  $\text{mg}/\text{m}^3$ ), indicating limitations in characterizing the most extreme blooms.

The MCMC traces (Fig. 6b) demonstrate good convergence of the parameter estimates, with stable chains and effective mixing properties. The stability of these traces provides confidence in the basic parameter estimates, even though the model struggles with the most extreme events. This paradox - good convergence but poor representation of the highest values - suggests that the statistical assumptions underlying the GEV framework may not fully capture the mechanisms driving exceptional blooms.

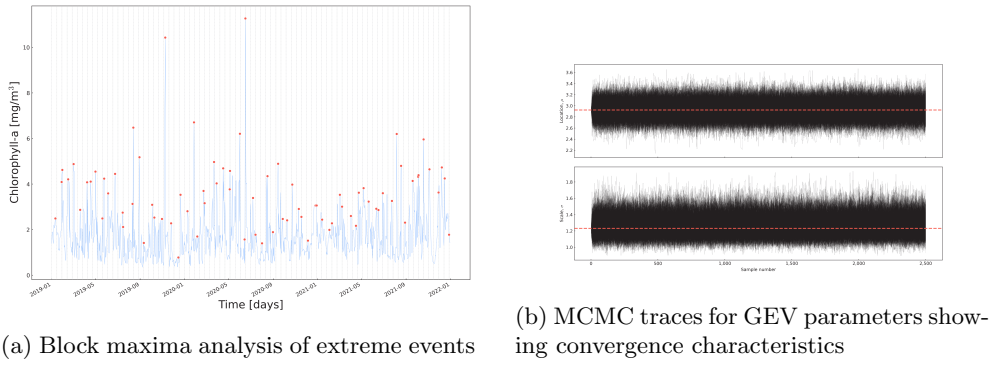


**Fig. 6:** Extreme value analysis results for chlorophyll-a concentrations

The block maxima analysis (Fig. 6a) reveals a systematic pattern in the occurrence of high-concentration events, but notably underestimates the magnitude of the two major HABs. This underestimation can be attributed to several factors: first, the assumption of regular extreme value behavior may not hold for biologically-driven extremes that involve complex feedbacks; second, the 14-day block size, while appropriate for capturing general patterns, may smooth out the most intense short-duration events; and third, the relatively short time series (3 years) limits the model's ability to characterize rare events robustly.

The diagnostic plots (Fig. 7) provide detailed evidence of the GEV model's performance and limitations. The return period plot (Fig. 7a) reveals significant deviation between observed and predicted values at the highest return periods, with the two major HAB events (11.270 and 10.430  $\text{mg}/\text{m}^3$ ) lying well above the model's predictions and their associated confidence intervals. This systematic underestimation of

extreme events suggests that these exceptional blooms may represent a different statistical regime or result from compound effects not captured by standard extreme value theory.

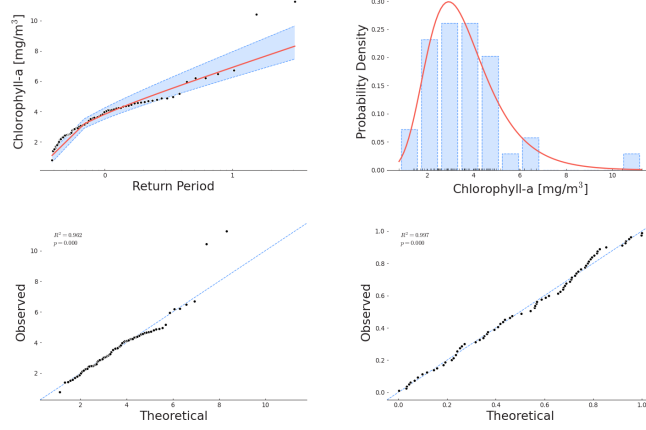


**Fig. 7:** Diagnostic plots for extreme value analysis: (a) Return period plot showing observed exceedances and model predictions with 95% confidence intervals, (b) Probability density function comparison between empirical and fitted distributions, (c) Q-Q plot for assessing model fit, and (d) P-P plot examining probability transformations. Two dots with the longest return periods in plot (a) indicate the two HAB events (11.270 and 10.430 mg/m<sup>3</sup>) that exceed model predictions

The probability density function comparison (Fig. 7b) demonstrates reasonable agreement between the fitted Gumbel distribution (location  $\mu = 2.924$ , scale  $\sigma = 1.231$ ) and empirical data for moderate extremes but shows clear divergence in the upper tail. This misfit is particularly evident in the Q-Q plot (Fig. 7c), where the departure from the diagonal line at high quantiles indicates that the chosen distribution family may not adequately represent the true probability structure of extreme chlorophyll-a events. The P-P plot (Fig. 7d) further confirms this pattern, showing systematic deviations in probability transformations for the highest values.

The failure of the GEV model to capture these extreme HABs can be attributed to several factors: First, the assumption of asymptotic behavior in classical extreme value theory may not hold for biologically-driven extremes that involve complex feedbacks and threshold responses. Second, the block maxima approach with a 14-day window, while appropriate for capturing the general structure of extremes, may not adequately represent the rapid development and intense nature of exceptional bloom events. Third, the relatively short time series (3 years) limits the model's ability to characterize very rare events reliably, particularly when these events may arise from unique combinations of environmental conditions.

### 3.5 Machine Learning Analysis and Environmental Controls

The AutoGluon machine learning analysis employed a WeightedEnsemble.L2 model that combines three base learners through the equation:

$$\hat{y} = 0.462f_{\text{ExtraTreesMSE}}(X) + 0.346f_{\text{CatBoost}}(X) + 0.192f_{\text{LightGBMXT}}(X) \quad (33)$$

where  $\hat{y}$  represents the predicted chlorophyll-a concentration and  $f_i(X)$  denotes each base model’s prediction given input features  $X$ . This weighted combination achieved moderate predictive performance (RMSE = 0.868 mg/m<sup>3</sup>, R<sup>2</sup> = 0.204) in capturing chlorophyll-a dynamics. The model’s architecture leverages the complementary strengths of each algorithm, with ExtraTreesMSE providing robust handling of non-linear relationships, CatBoost offering gradient-based optimization, and LightGBMXT capturing complex feature interactions.

The relative contributions of the base models (Table 1) demonstrate the dominance of ExtraTreesMSE (46.2%) in final predictions, followed by CatBoost (34.6%) and LightGBMXT (19.2%). This weighting structure suggests that non-linear relationships and complex interactions between environmental variables play crucial roles in determining chlorophyll-a concentrations [78]. The optimization of these weights through AutoGluon’s automated process ensures robust performance across different environmental conditions.

**Table 1:** Performance characteristics of base models in WeightedEnsemble.L2. The ensemble combines three complementary algorithms optimized for chlorophyll-a prediction

Model Component	Weight	Contribution (%)	Role in Ensemble
ExtraTreesMSE	0.462	46.2	Non-linear relationships
CatBoost	0.346	34.6	Gradient boosting
LightGBMXT	0.192	19.2	Feature interactions

The feature importance analysis (Table 2) reveals a clear hierarchy of environmental controls dominated by physical factors. Temperature emerges as the strongest predictor (0.072,  $p < 0.001$ ), followed by solar radiation (0.061,  $p = 0.002$ ) and phosphate (0.047,  $p < 0.001$ ), suggesting that phytoplankton biomass in Balikpapan Bay is primarily regulated by physical conditions, with nutrient availability playing a secondary but significant role. The moderate overall R<sup>2</sup> value (0.204) indicates that while these environmental parameters explain a significant portion of chlorophyll-a variability, other unmeasured factors likely contribute substantially to the system’s dynamics.

Critically, the trained model was serialized using pickle files, enabling potential future operational use for real-time predictions. This serialization preserves the exact state of the model, including all learned parameters, feature preprocessing steps,

**Table 2:** Environmental feature importance in chlorophyll-a prediction showing hierarchical influence of physical and chemical factors

Environmental Factor	Importance	p-value	Relative Contribution (%)
Temperature	0.072	<0.001	40.0
Solar Radiation	0.061	0.002	33.9
Phosphate	0.047	<0.001	26.1

and the weighted ensemble structure. The pickle files can be easily loaded for rapid deployment in operational monitoring systems:

```
import pickle
with open('model.pkl', 'rb') as f:
    model = pickle.load(f)
```

This approach ensures reproducibility and facilitates the model’s integration into automated monitoring systems. The serialized model can be regularly updated with new data, allowing for adaptive refinement of predictions as more observations become available. This capability is particularly valuable for developing early warning systems for HABs, where rapid assessment of environmental conditions is crucial for management responses.

The combination of moderate predictive performance ( $R^2 = 0.204$ ) and operational deployability through serialization suggests that while the model may not capture all aspects of chlorophyll-a variability, it provides a valuable tool for real-time monitoring and assessment. The ability to quickly process new environmental data and generate predictions could support adaptive management strategies, particularly during periods when conditions favor bloom development. Future improvements could focus on incorporating additional predictors, especially those related to water column stability and nutrient cycling, to enhance the model’s predictive capabilities while maintaining its operational utility.

## 4 Concluding Remarks

This study provides a comprehensive statistical analysis of chlorophyll-a dynamics in Balikpapan Bay, Indonesia, offering crucial insights into the functioning of this tropical coastal ecosystem in the context of ongoing urban development. Our multifaceted approach, combining classical time series analysis, extreme value modeling, and machine learning techniques, revealed complex temporal patterns and environmental drivers of phytoplankton biomass variability. The identification of key environmental drivers provides valuable guidance for ecosystem management in the face of climate change and urban development pressures associated with Indonesia’s new capital city development [2, 17]. Such understanding is particularly crucial given the bay’s strategic importance as a coastal area adjacent to the planned capital city of Nusantara.

The analysis of extreme events and seasonal patterns establishes a critical baseline for future monitoring efforts, particularly relevant for the detection and prediction of harmful algal blooms in tropical coastal systems [13, 34]. The observed non-Gaussian

distribution and the failure of standard extreme value approaches to capture major HABs suggest that exceptional bloom events arise from complex interactions not adequately represented by current statistical frameworks. This finding, combined with our machine learning results, indicates that while we can explain a significant portion of chlorophyll-a variability through measured environmental parameters, substantial uncertainty remains in predicting extreme events. The establishment of this model framework provides a foundation for real-time monitoring and early warning systems.

Several limitations of this study warrant consideration and point towards future research directions. The predictive performance of our models suggests the presence of unmeasured factors or complex non-linear interactions that current approaches cannot fully capture. Furthermore, the study period, while informative, may not fully capture long-term variability in the system. Future research should focus on incorporating additional environmental parameters, particularly those related to water column stability and nutrient cycling; developing specialized statistical frameworks for capturing extreme biological events; and extending the temporal coverage of observations to better understand long-term trends and climatological influences on phytoplankton dynamics in this rapidly changing coastal system.

**Acknowledgments.** We thank Andrew J. Ridgwell for insightful discussions on nutrient limitation dynamics in coastal ecosystems and Roby Douilly for valuable suggestions on time-series analysis.

**Code and Data availability.** The ocean color reanalysis data is available from CMEMS ([https://data.marine.copernicus.eu/product/OCEANCOLOUR\\_GLO\\_BGC\\_L4\\_MY\\_009\\_104](https://data.marine.copernicus.eu/product/OCEANCOLOUR_GLO_BGC_L4_MY_009_104)), biogeochemical and nutrient data (nitrate, phosphate, silicate, dissolved oxygen) from GLOBAL\_ANALYSIS\_FORECAST\_BIO\_001\_028 ([https://data.marine.copernicus.eu/product/GLOBAL\\_ANALYSISFORECAST\\_BGC\\_001\\_028](https://data.marine.copernicus.eu/product/GLOBAL_ANALYSISFORECAST_BGC_001_028)), river discharge data from GloFAS-ERA5 (<https://global-flood.emergency.copernicus.eu/>), ERA5 hourly data for solar radiation (<https://cds.climate.copernicus.eu/>), and precipitation data from BMKG Sepinggan station (<https://dataonline.bmkg.go.id>). All processed data and Python code used for the statistical analyses in this study are freely available at <https://github.com/sandyherho/BalikpapanBayChlStats>.

**Funding.** The financial support was provided by the Directorate General of Higher Education, Research, and Technology, Ministry of Education, Culture, Research, and Technology, Republic of Indonesia, under grant No.FITB.PN-1-12-202, and ITB's Research, Community Service and Innovation Program (PPMI-ITB) for the years 2021 and 2022, which supported the data collection and numerical modeling efforts. The data processing and statistical analysis aspects of this study were made possible through the Dean's Distinguished Fellowship at the University of California, Riverside 2023.

**Author Contributions.** I.P.A.: Conceptualization; Formal analysis; Methodology; Software; Writing – original draft. S.H.S.H.: Conceptualization; Formal analysis; Methodology; Software; Visualization; Writing – original draft. F.K.: Conceptualization; Formal analysis; Supervision; Writing – review & editing. M.R.P.: Supervision;



Writing – review & editing. S.C.S: Software; Writing – review & editing. All authors reviewed and approved the final version of the manuscript.

## Declarations

**Conflict of interest.** The authors declare there is no conflict.

**Competing interests.** Authors do not have any competing financial interest to declare.

**Consent to Publish.** Not Applicable

**Consent to Participate.** Not Applicable

**Ethics declaration.** Not Applicable

## References

- [1] Sekretariat Kabinet (SETKAB): The Law on the State Capital Marks the Beginning of the Construction of the National Capital Institute. National Cabinet Secretariat News (2022). <https://setkab.go.id/undang-undang-ibu-kota-negara-tandai-dimulainya-pembangunan-ikn/>
- [2] Putri, M.R., Anwar, I.P., Sihotang, Z., Bernawis, L.I., Setiawan, A., Riza, M., Mandang, I., Tatipatta, W.M.: Observation and numerical modeling of physical oceanography in the Balikpapan Bay, East Kalimantan: Preliminary results. *Depik* **10**(2), 130–135 (2021) <https://doi.org/10.13170/depik.10.2.19259>
- [3] Nurjaya, I.W., Surbakti, H., Hartanto, M.T., Gaol, J.L., Sulardi, A.: Water mass dynamics in Balikpapan Bay, Eastern Kalimantan Indonesia. *IOP Conf. Ser.: Earth Environ. Sci.* **176**(1), 012019 (2018) <https://doi.org/10.1088/1755-1315/176/1/012019>
- [4] Anwar, I.P., Putri, M.R., Tarya, A., Mandang, I.: Variation of water mass exchange on tidal scale in Balikpapan Bay. *IOP Conf. Ser. Earth Environ. Sci.* **925**(1), 012013 (2021) <https://doi.org/10.1088/1755-1315/925/1/012013>
- [5] Fauzah, S., Tarya, A., Ningsih, N.S.: Three-Dimensional Numerical Modelling of Tidal Current in Balikpapan Bay Using Delft 3D. *IOP Conf. Ser.: Earth Environ. Sci.* **925**(1), 012051 (2021) <https://doi.org/10.1088/1755-1315/925/1/012051>
- [6] Nur, A.A., Radjawane, I.M., Suprijo, T., Mandang, I.: Numerical Modeling of Currents Circulation in Balikpapan Bay during Oil Spill Event on March 31, 2018. *IOP Conf. Ser.: Earth Environ. Sci.* **618**(1), 012005 (2020) <https://doi.org/10.1088/1755-1315/618/1/012005>
- [7] Hermansyah, H., Ningsih, N.S., Nabil, N., Tarya, A., Syahrudin, S.: Numerical modeling of tidal current patterns using 3-Dimensional MOHID in Balikpapan

- Bay, Indonesia. *J. Ilmiah Perikanan dan Kelautan* **12**(1), 9–20 (2020) <https://doi.org/10.20473/jipk.v12i1.16257>.
- [8] Nurdianti, S., Khatizah, E., Najib, M.K., Hidayah, R.R.: Analysis of rainfall patterns in Kalimantan using fast fourier transform (FFT) and empirical orthogonal function (EOF). *J. Phys.: Conf. Ser.* **1796**(1), 012053 (2021) <https://doi.org/10.1088/1742-6596/1796/1/012053>
  - [9] Ramadhan, R., Marzuki, M., Suryanto, W., Sholihun, S., Yusnaini, H., Muharsyah, R., Hanif, M.: Trends in rainfall and hydrometeorological disasters in new capital city of Indonesia from long-term satellite-based precipitation products. *Remote Sens. Appl.: Soc. Environ.* **28**, 100827 (2022) <https://doi.org/10.1016/j.rsase.2022.100827>
  - [10] Effendi, H., Kawaroe, M., Lestari, D.F., Mursalin, M., Permadi, T.: Distribution of phytoplankton diversity and abundance in Mahakam Delta, East Kalimantan. *Procedia Environ. Sci.* **33**, 496–504 (2016) <https://doi.org/10.1016/j.proenv.2016.03.102>
  - [11] Zainol, Z., Akhir, M.F., Abdullah, N.S.: Hydrodynamics, nutrient concentrations, and phytoplankton biomass in a shallow and restricted coastal lagoon under different tidal and monsoonal environmental drivers. *Reg. Stud. Mar. Sci.* **38**, 101376 (2020) <https://doi.org/10.1016/j.rsma.2020.101376>
  - [12] Zhang, H., Wang, G., Zhang, C., Su, R., Shi, X., Wang, X.: Characterization of the development stages and roles of nutrients and other environmental factors in green tides in the Southern Yellow Sea, China. *Harmful Algae* **98**, 101893 (2020) <https://doi.org/10.1016/j.hal.2020.101893>
  - [13] Ho, K.C.: Overview of harmful algal blooms (red tides) in Hong Kong during 1975–2021. *J. Oceanogr. Limnol.* **40**(6), 2094–2106 (2022) <https://doi.org/10.1007/s00343-022-2205-z>
  - [14] Gade, M., Mayer, B., Meier, C., Pohlmann, T., Putri, M., Setiawan, A.: Oil pollution in Indonesian Waters: Combining statistical analyses of Envisat ASAR and SENTINEL-1A C-SAR Data with numerical tracer modelling. *Int. Arch. Photogramm. Remote Sens. Spatial Inf. Sci.* **42** (2017) <https://doi.org/10.5194/isprs-archives-XLII-3-W2-71-2017>
  - [15] Setiani, P., Ramdani, F.: Oil spill mapping using multi-sensor Sentinel data in Balikpapan Bay, Indonesia. In: 2018 4th International Symposium on Geoinformatics (ISyG), pp. 1–4 (2018). <https://doi.org/10.1109/ISYG.2018.8616119> . IEEE
  - [16] Zhang, Y., Zhao, T., Zhou, A., Zhang, Z., Liu, W.: Scenario Based Municipal Wastewater Estimation: Development and Application of a Dynamic Simulation Model. *Model. Simul. Eng.* **2016** (2016) <https://doi.org/10.1155/2016/1746310>

- [17] GEOHAB: Global ecology and oceanography of harmful algal blooms: harmful algal blooms in Asia. Technical report, IOC and SCOR, Paris and Newark, Delaware (2010)
- [18] Li, H., Chen, Y., Zhou, S., Wang, F., Yang, T., Zhu, Y., Ma, Q.: Change of dominant phytoplankton groups in the eutrophic coastal sea due to atmospheric deposition. *Sci. Total Environ.* **753**, 141961 (2021) <https://doi.org/10.1016/j.scitotenv.2020.141961>
- [19] Tarigan, M.S., Wiadnyana, N.N.: Monitoring of chlorophyll-a concentration using Terra-Aqua Modis Satellite imagery in Jakarta Bay. *J. Nas. Kelautan* **8**(2), 81–89 (2013)
- [20] Sidabutar, T., Srimariana, E.S., Wouthuyzen, S.: The potential role of eutrophication, tidal and climatic on the rise of algal bloom phenomenon in Jakarta Bay. *IOP Conf. Ser.: Earth Environ. Sci.* **429**(1), 012021 (2020) <https://doi.org/10.1088/1755-1315/429/1/012021>
- [21] Aditya, V., Koswara, A., Fitriya, N., Rachman, A., Sidabutar, T., Thoha, H.: Public awareness on harmful algal bloom (HAB) in Lampung Bay. *Mar. Res. Indones.* **38**(2), 71–75 (2015) <https://doi.org/10.14203/mri.v38i2.58>
- [22] Thoha, H., Muawanah, D., B.I.M., A., R., R., S.O., T., S., M., I., K., T., J.-C., A., E., M.: Resting cyst distribution and molecular identification of the harmful dinoflagellate *Margalefidinium polykrikoides* (Gymnodiniales, Dinophyceae) in Lampung Bay, Sumatra, Indonesia. *Front. Microbiol.* **10**, 306 (2019) <https://doi.org/10.3389/fmicb.2019.00306>
- [23] Mahmudi, M., Serihollo, L.G., Herawati, E.Y., Lusiana, E.D., Buwono, N.R.: A count model approach on the occurrences of harmful algal blooms (HABs) in Ambon Bay. *Egypt. J. Aquat. Res.* **46**(4), 347–353 (2020) <https://doi.org/10.1016/j.ejar.2020.08.002>
- [24] Likumahua, S., De Boer, M.K., Krock, B., Hehakaya, S., Imu, L., Müller, A., Max, T., Buma, A.G.J.: Variability of dinoflagellates and their associated toxins in relation with environmental drivers in Ambon Bay, eastern Indonesia. *Mar. Pollut. Bull.* **150**, 110778 (2020) <https://doi.org/10.1016/j.marpolbul.2019.110778>
- [25] Erickson, N., Mueller, J., Shirkov, A., Zhang, H., Larroy, P., Li, M., Smola, A.: AutoGluon-Tabular: Robust and accurate AutoML for structured data. arXiv preprint arXiv:2003.06505 (2020)
- [26] Shchur, O., Turkmen, A.C., Erickson, N., Shen, H., Shirkov, A., Hu, T., Wang, B.: AutoGluon-TimeSeries: AutoML for Probabilistic Time Series Forecasting. In: Faust, A., Garnett, R., White, C., Hutter, F., Gardner, J.R. (eds.) *Proceedings of the Second International Conference on Automated Machine Learning. Proceedings of Machine Learning Research*, vol. 224, pp. 9–121. PMLR, ??? (2023).

<https://proceedings.mlr.press/v224/shchur23a.html>

- [27] Anwar, I.P., Putri, M.R., Setiawan, A., Tarya, A., Mandang, I., Nurfitri, S., Tati-patta, W.M.: Detecting chlorophyll-a concentration and bloom patterns in the coastal area around Indonesia’s new capital city (Nusantara) using ocean color reanalysis data. *AACL Bioflux* **16**(4), 2349–2368 (2023)
- [28] E.U. Copernicus Marine Service Information: Global Ocean Colour (Copernicus-GlobColour), Bio-Geo-Chemical, L4 (monthly and interpolated) from Satellite Observations (1997-ongoing). [https://data.marine.copernicus.eu/product/OCEANCOLOUR.GLO\\_BGC\\_L4.MY\\_009\\_104/services](https://data.marine.copernicus.eu/product/OCEANCOLOUR.GLO_BGC_L4.MY_009_104/services) (2023)
- [29] Tozer, B., Sandwell, D.T., Smith, W.H.F., Olson, C., Beale, J.R., Wessel, P.: Global bathymetry and topography at 15 arc sec: SRTM15+. *Earth Space Sci.* **6**(10), 1847–1864 (2019) <https://doi.org/10.1029/2019EA000658>
- [30] Wessel, P., Luis, J.F., Uieda, L., Scharroo, R., Wobbe, F., Smith, W.H.F., Tian, D.: The Generic Mapping Tools version 6. *Geochem. Geophys. Geosyst.* **20**(11), 5556–5564 (2019) <https://doi.org/10.1029/2019GC008515>
- [31] IOCCG, Sathyendranath, S. (ed.): *Phytoplankton Functional Types from Space*. International Ocean-Colour Coordinating Group (IOCCG), Dartmouth, NS, Canada (2014). <https://doi.org/10.25607/OBP-106>
- [32] Miloslavich, P., Bax, N.J., Simmons, S.E., Klein, E., Appeltans, W., Aburto-Oropeza, O., Andersen Garcia, M., Batten, S.D., Benedetti-Cecchi, L., Checkley Jr, D.M., Chiba, S., Duffy, J.E., Dunn, D.C., Fischer, A., Gunn, J., Kudela, R., Marsac, F., Muller-Karger, F.E., Obura, D., Shin, Y.-J.: Essential ocean variables for global sustained observations of biodiversity and ecosystem changes. *Glob. Change Biol.* **24**(6), 2416–2433 (2018) <https://doi.org/10.1111/gcb.14108>
- [33] Kromkamp, J.C., Van Engeland, T.: Changes in phytoplankton biomass in the Western Scheldt Estuary during the period 1978–2006. *Estuaries Coasts* **33**(2), 270–285 (2010) <https://doi.org/10.1007/s12237-009-9215-3>
- [34] Blondeau-Patissier, D., Gower, J.F.R., Dekker, A.G., Phinn, S.R., Brando, V.E.: A review of ocean color remote sensing methods and statistical techniques for the detection, mapping and analysis of phytoplankton blooms in coastal and open oceans. *Prog. Oceanogr.* **123**, 123–144 (2014) <https://doi.org/10.1016/j.pocean.2013.12.008>
- [35] Barange, M., Merino, G., Blanchard, J.L., Scholtens, J., Harle, J., Allison, E.H., Allen, J.I., Holt, J., Jennings, S.: Impacts of climate change on marine ecosystem production in societies dependent on fisheries. *Nat. Clim. Change* **4**(3), 211–216 (2014) <https://doi.org/10.1038/nclimate2119>
- [36] Boyce, D.G., Lewis, M.R., Worm, B.: Global phytoplankton decline over the past

- p>century.
- Nature*
- 466**
- (7306), 591–596 (2010)
- <https://doi.org/10.1038/nature09268>
- [37] Harrigan, S., Zsoter, E., Alfieri, L., Prudhomme, C., Salamon, P., Wetterhall, F., Barnard, C., Cloke, H., Pappenberger, F.: GloFAS-ERA5 operational global river discharge reanalysis 1979–present. *Earth Syst. Sci. Data* **12**(3), 2043–2060 (2020) <https://doi.org/10.5194/essd-12-2043-2020>
  - [38] Lohrenz, S.E., Fahnenstiel, G.L., Redalje, D.G., Lang, G.A., Chen, X., Dagg, M.J.: Variations in primary production of northern Gulf of Mexico continental shelf waters linked to nutrient inputs from the Mississippi River. *Mar. Ecol. Prog. Ser.* **155**, 45–54 (1997) <https://doi.org/10.3354/meps155045>
  - [39] Ding, S., Chen, P., Liu, S., Zhang, G., Zhang, J., Dan, S.F.: Nutrient dynamics in the Changjiang and retention effect in the Three Gorges Reservoir. *J. Hydrol.* **574**, 96–109 (2019) <https://doi.org/10.1016/j.jhydrol.2019.04.034>
  - [40] E.U. Copernicus Marine Service Information: Global Ocean Biogeochemistry Analysis and Forecast. [https://data.marine.copernicus.eu/product/GLOBAL\\_ANALYSISFORECAST\\_BGC\\_001\\_028](https://data.marine.copernicus.eu/product/GLOBAL_ANALYSISFORECAST_BGC_001_028) (2023)
  - [41] Moore, C.M., Mills, M.M., Arrigo, K.R., Berman-Frank, I., Bopp, L., Boyd, P.W., Galbraith, E.D., Geider, R.J., Guieu, C., Jaccard, S.L., Jickells, T.D., Roche, J.L., Lenton, T.M., Mahowald, N.M., Marañón, E., Marinov, I., Moore, J.K., Nakatsuka, T., Oschlies, A., Saito, M.A., Thingstad, T.F., Tsuda, A., Ulloa, O.: Processes and patterns of oceanic nutrient limitation. *Nat. Geosci.* **6**(9), 701–710 (2013) <https://doi.org/10.1038/ngeo1765>
  - [42] Pasquier, B., Holzer, M., Chamberlain, M.A., Matear, R.J., Bindoff, N.L., Primeau, F.W.: Optimal parameters for the ocean’s nutrient, carbon, and oxygen cycles compensate for circulation biases but replumb the biological pump. *Biogeosciences* **20**(14), 2985–3009 (2023) <https://doi.org/10.5194/bg-20-2985-2023>, 2023
  - [43] Hersbach, H., Bell, B., Berrisford, P., Biavati, G., Horányi, A., Muñoz Sabater, J., Nicolas, J., Peubey, C., Radu, R., Rozum, I., *et al.*: ERA5 hourly data on single levels from 1940 to present. Copernicus Clim. Change Serv. (C3S) Clim. Data Store (CDS) (2023) <https://doi.org/10.24381/cds.adbb2d47>
  - [44] Kirk, J.T.O.: *Light and Photosynthesis in Aquatic Ecosystems*, 3rd edn. Cambridge University Press, ??? (2010)
  - [45] Falkowski, P.G., Raven, J.A.: *Aquatic Photosynthesis*, 2nd edn. Princeton University Press, ??? (2007)
  - [46] Pusat Database BMKG: Online Data Database Center for Indonesian Meteorology, Climatology and Geophysics Agency. <https://dataonline.bmkg.go.id/> (2023)

- [47] Townsend, D.W., Rebeck, N.D., Thomas, M.A., Karp-Boss, L., Gettings, R.M.: Oceanography of the northwest Atlantic continental shelf. *Sea: The Global Coastal Ocean: Interdisciplinary Regional Studies and Syntheses* **13**, 119–168 (2010)
- [48] Zhou, W., Gao, J., Liao, J., Shi, R., Li, T., Guo, Y., Long, A.: Characteristics of Phytoplankton Biomass, Primary Production and Community Structure in the Modaomen Channel, Pearl River Estuary, with Special Reference to the Influence of Saltwater Intrusion during Neap and Spring Tides. *PloS One* **11**(12), 0167630 (2016) <https://doi.org/10.1371/journal.pone.0167630>
- [49] Cloern, J.E., Abreu, P.C., Carstensen, J., Chauvaud, L., Elmgren, R., Grall, J., Greening, H., Johansson, J.O.R., Kahru, M., Sherwood, E.T., *et al.*: Human activities and climate variability drive fast-paced change across the world’s estuarine–coastal ecosystems. *Global Change Biol.* **22**(2), 513–529 (2016) <https://doi.org/10.1111/gcb.13059>
- [50] Carstensen, J., Conley, D.J., Almroth-Rosell, E., Asmala, E., Bonsdorff, E., Fleming-Lehtinen, V., Gustafsson, B.G., Gustafsson, C., Heiskanen, A.S., Janas, U., *et al.*: Factors regulating the coastal nutrient filter in the Baltic Sea. *Ambio* **49**(6), 1194–1210 (2020) <https://doi.org/10.1007/s13280-019-01282-y>
- [51] Cloern, J.E.: Phytoplankton bloom dynamics in coastal ecosystems: a review with some general lessons from sustained investigation of San Francisco Bay, California. *Rev. Geophys.* **34**(2), 127–168 (1996) <https://doi.org/10.1029/96RG00986>
- [52] Zingone, A., Escalera, L., Aligizaki, K., Fernández-Tejedor, M., Ismael, A., Montresor, M., *et al.*: Toxic marine microalgae and noxious blooms in the Mediterranean Sea: A contribution to the Global HAB Status Report. *Harmful Algae* **102**, 101843 (2021) <https://doi.org/10.1016/j.hal.2020.101843>
- [53] Zwillinger, D., Kokoska, S.: CRC Standard Probability and Statistics Tables and Formulae, Student Edition. CRC Press, ??? (2000)
- [54] Cabrera, S., López, M., Tartarotti, B.: Phytoplankton and zooplankton response to ultraviolet radiation in a high-altitude Andean lake: short-versus long-term effects. *J. Plankton Res.* **19**(11), 1565–1582 (1997) <https://doi.org/10.1093/plankt/19.11.1565>
- [55] Joanes, D.N., Gill, C.A.: Comparing measures of sample skewness and kurtosis. *J. R. Stat. Soc. Ser. D Stat.* **47**(1), 183–189 (1998) <https://doi.org/10.1111/1467-9884.00122>
- [56] Platt, T., Sathyendranath, S.: Ecological indicators for the pelagic zone of the ocean from remote sensing. *Remote Sens. Environ.* **112**(8), 3426–3436 (2008) <https://doi.org/10.1016/j.rse.2007.10.016>

- [57] Shapiro, S.S., Wilk, M.B.: An analysis of variance test for normality (complete samples). *Biometrika* **52**(3/4), 591–611 (1965) <https://doi.org/10.1093/biomet/52.3-4.591>
- [58] D’Agostino, R.B.: Transformation to normality of the null distribution of  $g_1$ . *Biometrika* **57**(3), 679–681 (1970) <https://doi.org/10.1093/biomet/57.3.679>
- [59] Zar, J.H.: *Biostatistical Analysis*. Pearson Education India, ??? (2014)
- [60] Dickey, D.A., Fuller, W.A.: Distribution of the estimators for autoregressive time series with a unit root. *J. Am. Stat. Assoc.* **74**(366a), 427–431 (1979) <https://doi.org/10.1080/01621459.1979.10482531>
- [61] Kwiatkowski, D., Phillips, P.C., Schmidt, P., Shin, Y.: Testing the null hypothesis of stationarity against the alternative of a unit root: How sure are we that economic time series have a unit root? *J. Econom.* **54**(1-3), 159–178 (1992) [https://doi.org/10.1016/0304-4076\(92\)90104-Y](https://doi.org/10.1016/0304-4076(92)90104-Y)
- [62] Cazelles, B., Chavez, M., Berteaux, D., Ménard, F., Vik, J.O., Jenouvrier, S., Stenseth, N.C.: Wavelet analysis of ecological time series. *Oecologia* **156**(2), 287–304 (2008) <https://doi.org/10.1007/s00442-008-0993-2>
- [63] Box, G.E., Jenkins, G.M., Reinsel, G.C., Ljung, G.M.: *Time Series Analysis: Forecasting and Control*. John Wiley & Sons, ??? (2015)
- [64] Scheffer, M., Carpenter, S., Foley, J.A., Folke, C., Walker, B.: Catastrophic shifts in ecosystems. *Nature* **413**(6856), 591–596 (2001) <https://doi.org/10.1038/35098000>
- [65] Sugihara, G., May, R.M.: Nonlinear forecasting as a way of distinguishing chaos from measurement error in time series. *Nature* **344**(6268), 734–741 (1990) <https://doi.org/10.1038/344734a0>
- [66] Coles, S.: *An Introduction to Statistical Modeling of Extreme Values*. Springer, London (2001)
- [67] Herho, S.H.S.: A Univariate Extreme Value Analysis and Change Point Detection of Monthly Discharge in Kali Kupang, Central Java, Indonesia. *JOIV: International Journal on Informatics Visualization* **6**(4), 862–868 (2022) <https://doi.org/10.30630/joiv.6.4.953>
- [68] Anderson, D.M., Glibert, P.M., Burkholder, J.M.: Harmful algal blooms and eutrophication: nutrient sources, composition, and consequences. *Estuaries* **25**(4), 704–726 (2002) <https://doi.org/10.1007/BF02804901>
- [69] G. Bocharov: pyextremes: Extreme Value Analysis (EVA) in Python. <https://georgebv.github.io/pyextremes/>

- [70] Stephenson, A.G., Tawn, J.A.: Bayesian Inference for Extremes: Accounting for the Three Extremal Types. *Extremes* **7**(4), 291–307 (2004) <https://doi.org/10.1007/s10687-004-3479-6>
- [71] Hallegraeff, G.M.: Ocean climate change, phytoplankton community responses, and harmful algal blooms: a formidable predictive challenge. *J. Phycol.* **46**(2), 220–235 (2010) <https://doi.org/10.1111/j.1529-8817.2010.00815.x>
- [72] Olden, J.D., Lawler, J.J., Poff, N.L.: Machine Learning Methods Without Tears: A Primer for Ecologists. *Q. Rev. Biol.* **83**(2), 171–193 (2008) <https://doi.org/10.1086/587826>
- [73] Hastie, T., Tibshirani, R., Friedman, J.: *The Elements of Statistical Learning: Data Mining, Inference, and Prediction*. Springer, ??? (2009)
- [74] Willmott, C.J., Matsuura, K.: Advantages of the mean absolute error (MAE) over the root mean square error (RMSE) in assessing average model performance. *Clim. Res.* **30**(1), 79–82 (2005) <https://doi.org/10.3354/cr030079>
- [75] Breiman, L.: Random Forests. *Machine Learning* **45**(1), 5–32 (2001) <https://doi.org/10.1023/A:1010933404324>
- [76] Beaugrand, G., Kirby, R.R.: How Do Marine Pelagic Species Respond to Climate Change? Theories and Observations. *Annu. Rev. Mar. Sci.* **10**, 169–197 (2018) <https://doi.org/10.1146/annurev-marine-121916-063304>
- [77] Halpern, B.S., Frazier, M., Afflerbach, J., Lowndes, J.S., Micheli, F., O’Hara, C., Scarborough, C., Selkoe, K.A.: Recent pace of change in human impact on the world’s ocean. *Sci. Rep.* **9**(1), 11609 (2019) <https://doi.org/10.1038/s41598-019-47201-9>
- [78] Kwon, Y.S., Baek, S.H., Lim, Y.K., Pyo, J.-C., Ligaray, M., Park, Y., Cho, K.H.: Monitoring Coastal Chlorophyll-a Concentrations in Coastal Areas using Machine Learning Models. *Water* **10**(8), 1020 (2018) <https://doi.org/10.3390/w10081020>
- [79] Bi, H., Song, J., Zhao, J., Liu, H., Cheng, X., Wang, L., Cai, Z., Benfield, M.C., Otto, S., Goberville, E., Keister, J., Yang, Y., Yu, X., Cai, J., Ying, K., Conversi, A.: Temporal characteristics of plankton indicators in coastal waters: High-frequency data from PlanktonScope. *J. Sea Res.* **189**, 102283 (2022) <https://doi.org/10.1016/j.seares.2022.102283>
- [80] Liu, H., Wu, C., Xu, W., Wang, X., Thangaraj, S., Zhang, G., Zhang, X., Zhao, Y., Sun, J.: Surface Phytoplankton Assemblages and Controlling Factors in the Strait of Malacca and Sunda Shelf. *Front. Mar. Sci.* **7**, 33 (2020) <https://doi.org/10.3389/fmars.2020.00033>



- [81] Pourzangbar, A., Jalali, M., Brocchini, M.: Machine learning application in modelling marine and coastal phenomena: a critical review. *Front. Environ. Eng.* **2**, 1235557 (2023) <https://doi.org/10.3389/fenve.2023.1235557>
- [82] Srichandan, S., Baliarsingh, S.K., Prakash, S., Lotliker, A.A., Parida, C., Sahu, K.: Seasonal dynamics of phytoplankton in response to environmental variables in contrasting coastal ecosystems. *Environ. Sci. Pollut. Res. Int.* **26**, 12025–12041 (2019) <https://doi.org/10.1007/s11356-019-04569-5>
- [83] Carstensen, J., Klais, R., Cloern, J.E.: Phytoplankton blooms in estuarine and coastal waters: Seasonal patterns and key species. *Estuar. Coast. Shelf Sci.* **162**, 98–109 (2015) <https://doi.org/10.1016/j.ecss.2015.05.005>